AIAA JOURNAL
Vol. 45, No. 11, November 2007

Optical Diagnostics Applied to a Gas Turbine Pilot Burner

H. Seyfried,* C. Brackmann,† A. Lindholm,† and M. Linne‡
Lund University, S-221 00, Lund, Sweden
F. Barreras§
Laboratory for Research in Combustion Technology/Spanish National Research Council, 50018 Zaragoza, Spain
and
R. v.d. Bank¶
Rolls–Royce Deutschland, Ltd. & Company KG, 15827 Blankenfelde-Mahlow, Germany

DOI: 10.2514/1.30032

This paper presents the application of several optical measurement techniques for the characterization of the combustion behavior of the pilot burner of a gas turbine combustor developed according to the lean premixed prevaporized concept. The vaporization of the kerosene fuel (Jet-A) injected by a pilot spray and its consequent mixing with air has been visualized using combined laser-induced fluorescence and Mie scattering measurements. The laser-induced fluorescence/Mie measurements can be used to estimate the length and time scales for evaporation and mixing with air of kerosene (Jet-A) for the lean, premixed, and prevaporized pilot burner. In addition, the feasibility of using laser-induced incandescence for soot characterization has been investigated. Finally, spontaneous flame emission (i.e., chemiluminescence and thermal radiation) have been measured providing information on the overall characteristics of the combustion.

Nomenclature

M_{air}	=	mass flow air
P	=	pressure
T	=	temperature
W_{fuel}	=	mass flow fuel
ϕ	=	equivalence ratio

I. Introduction

THE demand for high efficiency in combination with ultralow emissions from combustion driven devices has propelled the design, development, and incorporation of special combustion concepts. One of the driving forces is the reduction of NO_x emission levels to their minimum. Example designs to meet this requirement include the rich burn, quick quench, lean burn (RQL) and the lean, premixed, prevaporized (LPP) concepts [1]. In the latter case the liquid fuel is vaporized and a preheated fuel/air mixture with a strong excess of air is generated within the duct. To achieve optimum combustion over the entire turndown range, special care has to be taken to optimize the degree of vaporization and to stabilize the flame in a recirculation zone produced by a strongly swirling flowfield. An additional restriction is that the residence time of the fuel/air mixture in the premix duct must be minimized to avoid flashback. Moreover, lean premixed flames can be subject to thermoacoustic instabilities that have the potential to cause liner damage. One way to avoid this problem is to provide a nonpremixed pilot flame by a centrally integrated pilot fuel injector and V shroud flame stabilizer [2,3]. In such a case, however, the pilot flame is often the major source of NO emissions. Careful design of the pilot is thus critical for a piloted LPP duct. In the present work, therefore, several optical techniques were applied for characterization of the combustion behavior of a centrally placed pilot burner equipped with a pressure–swirl atomizer and V shroud flame stabilizer.

Advanced computational and experimental tools have proven invaluable for the development of modern combustor ducts like the one just described. Among the advanced experimental tools, nonintrusive, spatially and temporally resolved laser diagnostic techniques have made it possible to observe most of the thermal/fluid and chemical dynamics of interest in such flows [4,5].

Investigations of fuel/air mixtures using laser-based methods have been carried out for many years [5]. Often measurements are made using model fuels, for example, one- or two-component fuels with a seeding species with known optical properties added to the fuel [5,6]. However, such an approach may not always mimic the real situation with the practical fuel. Thus, in situations where the degree of vaporization is of crucial importance for optimum performance it is more realistic to use liquid multicomponent fuels. For laser-based investigation of the degree of vaporization, two-phase diagnostics must be applied. This area is not as developed as diagnostics directed toward a single phase, despite its industrial importance. One alternative for two-phase diagnostics is based on the addition of so-called Exciplex tracer compounds to a model fuel [7–9]. The Exciplex compounds exhibit laser-induced fluorescence in different spectral regions depending on whether they are bound to liquid droplets or are in gas phase. The Exciplex fluorescence technique is based on the use of model fuels, which are subject to the drawbacks already mentioned. In addition it has also been found that the fluorescence is strongly quenched by oxygen, making the technique less suitable for studies of lean fuel/air mixtures.

Another alternative, but nonquantitative, technique for two-phase visualization is to combine laser-induced fluorescence (LIF) and Mie scattering. Mie scattering is simply elastic scattering of radiation from larger particles and droplets, and its detection is therefore a suitable indicator of the liquid phase of the fuel. Furthermore, complex multicomponent hydrocarbon fuels, such as the kerosene

Presented as Paper 0469 at the 45th AIAA Aerospace Sciences Meeting and Exhibit, Reno, Nevada, 8–11 January 2007; received 26 January 2007; revision received 20 April 2007; accepted for publication 31 May 2007.

*Ph.D. Student, Division of Combustion Physics, Faculty of Engineering LTH.
†Ph.D., Division of Combustion Physics, Faculty of Engineering LTH.
‡Adjunct Professor, Division of Combustion Physics, Faculty of Engineering LTH.
§Ph.D.
¶Ph.D., Combustion Engineer Specialist.

(Jet-A) used in this application, can exhibit laser-induced fluorescence when excited by radiation in the ultraviolet spectral region, allowing the fluorescence signal to be used as an indicator of vaporized fuel. Two-phase studies using combined fluorescence and Mie scattering have been carried out in fundamental spray studies [10], combustion engine applications [11,12], and also for investigation of gas turbine combustors [13,14].

Soot formation and emission is an issue in many combustion processes. For gas turbine combustors operating according to the LPP concept (lean combustion), soot emissions should be low. The experiments presented in this paper, however, deal with the pilot burner of an LPP module [2,3]. The rich pilot flames (without main fuel injection) investigated are all nonpremixed and they clearly exhibit formation of soot. Laser-induced incandescence (LII) is a laser diagnostic method for visualization of the soot distribution [5]. The technique is based on the detection of emitted blackbody radiation following instantaneous heating of the soot particles, by absorption of laser radiation, to temperatures around 4000 K. In combination with calibration measurements and data evaluation using a soot particle model the method allows parameters such as soot volume fraction and soot particle size distributions to be quantified [5]. The LII measurements carried out in the present work explored the potential of the LII technique in a pilot burner configuration under pressure and to provide qualitative information of soot distribution in the combustion zone. The technique has previously been demonstrated in the reaction zone of a model gas turbine combustor [15]. In previous work, Meier et al. [16] reported on fuel, temperature, and OH distributions in a model combustor at elevated pressure, and Meyer et al. [17] reported on soot characteristics, OH, and droplet Mie scattering in a swirl-stabilized spray flame at atmospheric pressure. Here, we describe fuel visualization in terms of gas phase/droplet distributions using simultaneous LIF/Mie scattering, respectively, and soot characteristics in a pressurized combustor with Jet-A as fuel.

II. Experimental

A. High-Pressure Rig and LP(P)4 Pilot Burner

The measurements presented in this paper were carried out in an experimental rig designed for combustion tests at high pressure at Lund University [2]. The test rig allows a maximum airflow rate of 1.3 kg/s at inlet temperature and pressure up to 650 K and 16 bar, respectively. Liquid fuel can be supplied at a rate of 100 kg/h corresponding to 1 MW burner input and for natural gas the capacity is up to 86 kg/h ($\approx$1 MW) with a maximum pressure of 13 bar. The high-pressure test rig is designed for investigation of combustion phenomena, to provide data for validation of combustion models, and for development of new diagnostic methods. The scale of the facility ensures that experimental studies can be performed up to industrially relevant size and conditions.

The schematic setup for the air and fuel flows during the measurements can be seen in Fig. 1. Air for the facility is compressed up to 16 bar by a 750 kW air compressor located in a separate module. The air supplied from the compressor is introduced to the test section in an outer pressure vessel, and it acts as cooling air for the combustion chamber. A small amount of the air is also used for film cooling of the inner wall of the quartz windows of the combustion chamber. Most of the air, however, flows toward the right in Fig. 1 (inside the annulus of the outer pressure vessel), toward the electric preheater which heats the air up to a maximum of 650 K. The amount of air introduced to the facility is controlled with a computer-controlled bypass valve deriving an error signal from a mass flow meter with the compressor running at constant speed. The excess air is exhausted through the flue. All of the air that exits the electric preheater flows into the inner pipe of the annulus into the combustion duct.

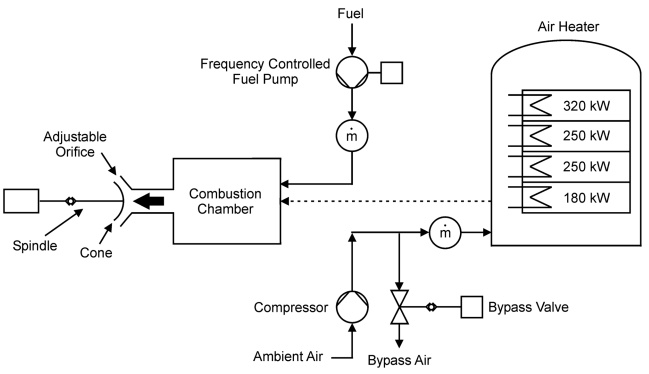

Fig. 1 Schematic of the air- and fuel flow in the rig during the measurements, the dashed line denotes the inner pipe of the annulus.

The combustion chamber has a square cross section and is equipped with quartz windows to provide optical access. The inner window set is designed primarily to deal with high temperatures. The outer wall contains the pressure and is also fitted with quartz windows. Optical- and laser-based diagnostic measurements are performed through the window sets. Combustion can occur within various ducts that are mounted inside the optically accessible, 10 cm $\times$ 10 cm housing. The unit has two lines of fuel supply for liquid fuel: one intended for the pilot burner and the other for the main burner. These can be operated simultaneously but in the present experiments only the pilot burner was used and therefore only one of the fuel supply lines was needed. The amount of fuel, in this case kerosene Jet-A, is computer controlled via the fuel pump. Combustion products then pass through an adjustable, choked-flow orifice, which controls the chamber pressure and the pressure drop down to $\sim$1 bar downstream. Water jets cool the combustion products and they flow out of the exhaust system mounted on the roof. In addition to these facilities, the rig has fully automated control and safety systems.

The particular combustor duct used in this work is one in a series of aeroengine LPP injectors designed and tested by Rolls–Royce Deutschland [2,3]. Just one injector from the fourth of the development series [denoted LP(P)4,] is shown in Fig. 2. It is a relatively short duct with small residence times, a high swirl induced by a series of axial blades, and a pilot flame that is stabilized by an integral V shroud. The channels formed by the axial blades contain the main fuel injectors which were not used in this study. The pilot injector is a pressure–swirl atomizer with interchangeable nozzles that achieve various spray cone angles. A spray angle around 45 deg was used in this work for easier ignition near the wall, although it may have contributed to some window fouling problems as well.

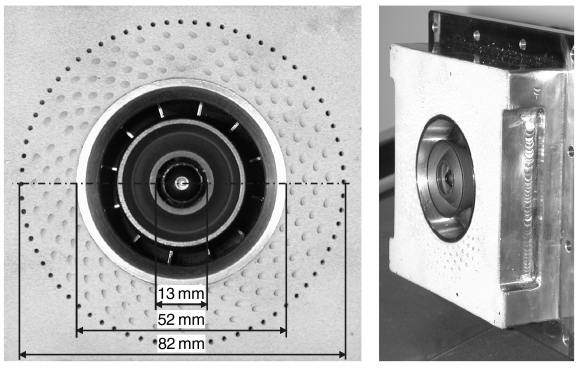

Fig. 2 Photo of the Rolls–Royce Deutschland's LPP(4) module with integrated pilot burner. The duct is mounted in an effusion cooling plate with a thermal barrier coating. a) End-on photo. Note that the duct itself is 52 mm in diameter while the effusion cooling array extends out to 82 mm diameter. The pilot injector is on center, surrounded by the V shroud (with inner diameter = 13 mm), which is surrounded by the swirlers in the main duct (not fueled during the experiments). b) Mounting plate viewed at an angle, emphasizing the V shroud flame stabilizer.

B. Simultaneous LIF and Mie Scattering

The second and fourth harmonic of a Q-switched Nd:YAG laser (Quantel YG-581C) at 532 and 266 nm, respectively, were used for the generation of the Mie scattering and LIF signals. The laser system produces pulses having a duration of 10 ns at a repetition rate of 10 Hz. The output pulse energy obtained at 532 nm was approximately 320 mJ. In Fig. 3 the experimental setup for the combined LIF and Mie scattering experiments is shown. A similar experimental approach for two-phase visualization has formerly been reported in [13,14]. The main part of the 532 nm radiation was frequency doubled to obtain 266 nm for the LIF measurements, while about 5% was directed into a separate beam path to be used directly for the Mie scattering process. The laser pulse energy obtained at 266 nm was approximately 25 mJ. The 532 nm beam, separated by a dichroic beam splitter, was directed through a variable attenuator in order to adjust the Mie scattering signal level by means of the beam intensity. The 266 nm beam and the attenuated 532 nm beam were overlapped by use of a dichroic mirror reflecting the 266 nm beam and transmitting the 532 nm beam. The beams propagated together through the combustion chamber. Two horizontal laser sheets with a thickness of about 0.5 mm were created by use of an $f = -40$ mm cylindrical and an $f = +300$ mm spherical lens. The sheet width was approximately 35 mm, with edges that were clipped before the entrance to the combustion chamber to generate a more homogeneous laser profile. The foci of the laser sheets were positioned inside the combustion chamber on the centerline in front of the LP(P)4 pilot nozzle. The generated signals were detected perpendicular to the laser sheets through a window mounted on top of the combustion chamber, via an aluminum mirror. An intensified charge-coupled device (CCD) camera (Princeton Instruments IMAX 512×512 pixels) equipped with an UV Nikkor $f = 105$ mm lens, $f/4.5$, was used for the detection and an area of about 85×40 mm^2 was depicted. The gate width of the detector was set to 100 ns. An image separator (a stereoscope) was placed in front of the CCD camera to enable two images of the measurement region to be obtained simultaneously on the CCD chip. A 532 nm interference

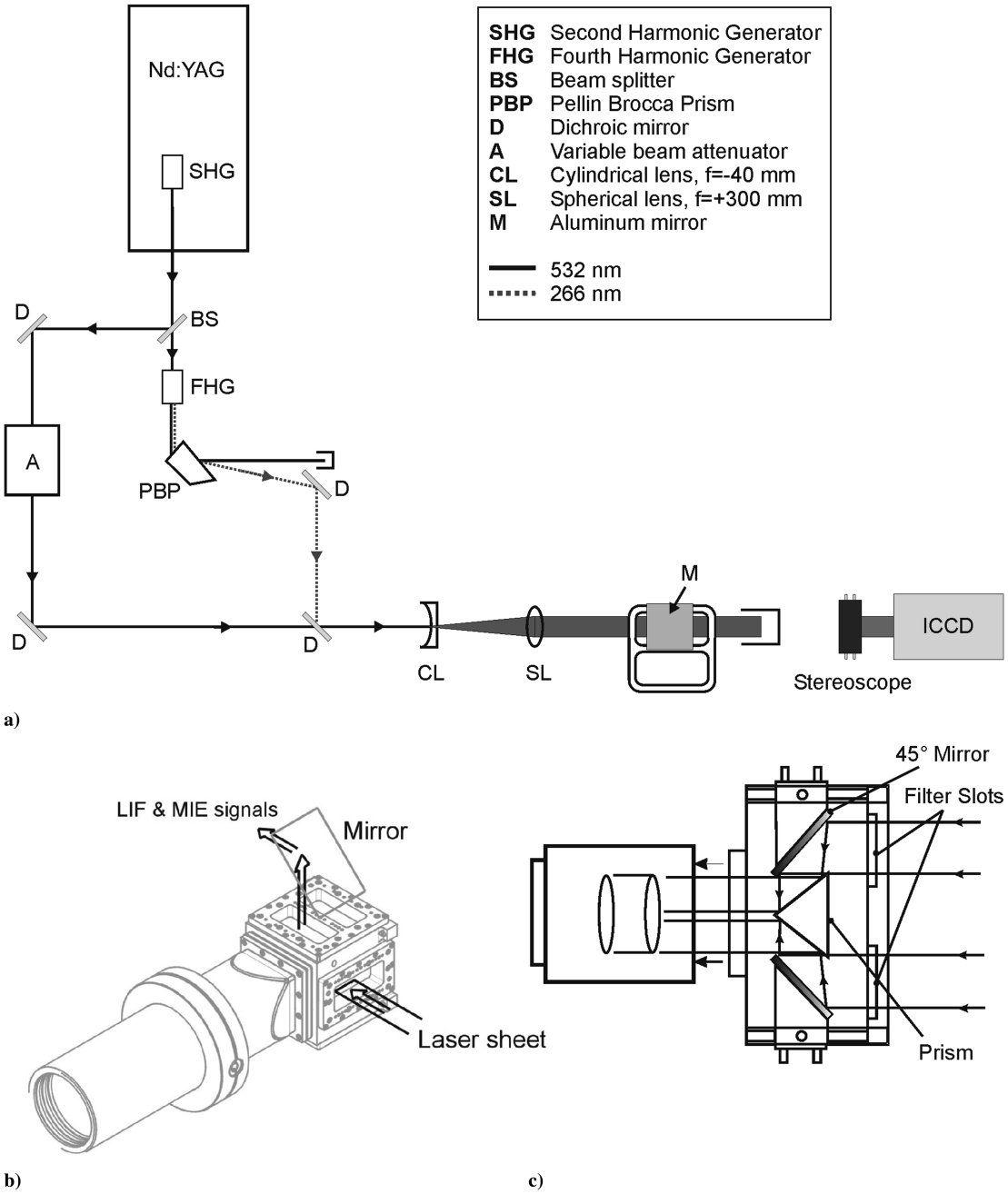

Fig. 3 a) Schematic of the experimental setup for the combined Mie scattering and LIF experiments. b) The arrangement of the laser sheets entering the combustion chamber and the setup for signal detection. c) Schematic of the stereoscope used for signal detection.

filter was inserted in one of the channels of the stereoscope to assure that only 532 nm scattering was detected in this channel. Two Schott filters, WG295 long-pass filter and BG3 color filter resulting in a spectral transmittance range from about 300 to 450 nm, were used in the second channel to assure that only fluorescence from the fuel was detected in this channel. Flame luminescence images detected without the lasers were used to subtract the interference from background radiation on the Mie scattering and LIF signals. The laser sheet arrangement in the combustion chamber and the stereoscope are illustrated in Figs. 3b and 3c.

The combined Mie scattering and LIF experiments were supplemented by a spectral study of the LIF signal. The purpose of this investigation was merely to measure the fluorescence emission when exciting the fuel with laser radiation at 266 nm rather than to achieve a deep spectroscopic understanding of the commercially available fuel. The fourth harmonic of the Nd:YAG laser (266 nm) was used as an excitation source and a horizontal sheet was created using the same optics as described previously. The sheet was focused in the center of the chamber close to the duct outlet. A spectrograph (Acton SP 150), $f/4$, with a grating of 300 lines/mm, was used in combination with an ICCD for signal detection. The fluorescence signal from a region dominated by the vapor phase was imaged onto the slit of the spectrometer.

C. Soot Visualization Using LII

For the LII experiments the second harmonic of the Nd:YAG laser at 532 nm, with approximate pulse energy of 140 mJ, was used to generate the LII signal. To gain two-dimensional information of the soot distribution the laser beam was formed into a narrow sheet using the same optics as in the fuel investigations. The laser sheet was directed into the combustion chamber through a window and focused in the center of the chamber close to the LP(P)4 pilot fuel nozzle. The LII signal was detected by the ICCD using a 100 ns gate width and a pulse delay of 210 ns. As in the Mie scattering and LIF study the signal was collected perpendicular to the laser sheet through the top window of the combustion chamber. Two optical filters were mounted in front of the camera, a short-pass filter with a cutoff wavelength at 450 nm and a BG3 color filter. This filter combination eliminates laser scattering at 532 nm and provides a good transmission in the spectral range between 300 and 450 nm.

III. Results and Discussion

A major issue during these measurements was the deposition of unburned fuel and soot on the quartz windows. This was likely due to the wide spray angle combined with the fact that the window cooling system is perhaps too effective. The strategy therefore became to ignite at a lean condition, make the laser measurements before deposits accumulated at the windows, proceed to a richer condition at a higher temperature, and go toward leaner conditions in steps for as long as the windows remained clear. In this way it was possible to perform laser-based measurements at two different global air fuel ratios (AFR). The operating conditions for the two cases are presented in Table 1. Point 1 represents the ignition condition.

The AFR values presented in the table are based on mass flow rates. Given that the jet flame studied is overall nonpremixed, the equivalence ratios are approximate values based on the overall fuel and airflows.

In Fig. 4 instantaneous images of the flame deduced from video recordings are shown. The images correspond to the operating conditions for which laser diagnostic measurements were performed. The upper images show the top view of the combustion chamber (same view as the CCD camera used for detection of the LIF/Mie and LII signals) and the lower images show the side view of the combustion chamber. The flow direction is from right to left in the images.

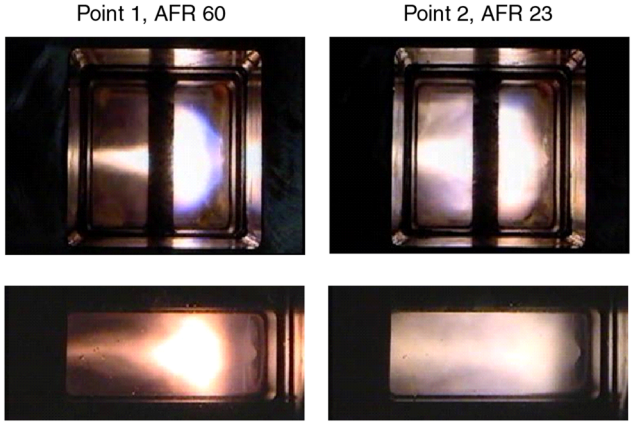

Fig. 4 Flame images corresponding to the operating conditions for which optical diagnostic measurements were performed. Top: Top view of the combustion chamber (same view as for the LIF/Mie and LII images). Bottom: Side view of the combustion chamber.

Rolls–Royce Deutschland's LP(P)4 duct used here had the same internal structure as a complete LPP duct (but no fuel flow to the main injectors), meaning that there was a set of swirler blades inside the air duct and these imparted a strong swirl to the airflow. In the images, therefore, one can see the effect of a flow recirculation on the flame at the midpoint of the chamber. In addition, one can see the flow narrow down to pass into the exit orifice on the centerline at the left wall in the images.

A. Flame Emission Measurements

The flames of the pilot burner under the running conditions provided in Table 1 showed moderate levels of blackbody radiation, which is apparent from the flames visible in the photos in Fig. 4. This characteristic of the rich pilot flames can also be observed in spectral measurements of the flame luminescence using the spectrometer and CCD described in the experimental section. The measurement volume was located in the center of the chamber close to the duct outlet, perpendicular to the flow direction. In Fig. 5 the flame emission spectrum for the running condition of AFR 60 is presented.

In the spectrum a broad and continuous spectral emission is obtained, mainly because of thermal radiation from the soot present owing to the nonpremixed characteristics of the combustion process. However, emission peaks at 309, 390, 431, and 473 nm are also observable, originating from the chemical processes involving excited OH, CH, and C_2 radicals. Chemiluminescence from those radicals is mainly produced in premixed combustion regions, which can be seen as the less luminous emission at the leading edge of the flame in the top view photo detected for AFR 60 in Fig. 4.

B. Simultaneous LIF and Mie Scattering

As an initial study to the fuel imaging measurements, the fluorescence signal obtained using 266 nm excitation was studied spectrally resolved. The LIF spectrum detected for the run condition of AFR 60 is presented in Fig. 6.

As can be seen in the figure, the fluorescence signal covers a rather broad spectral range, from approximately 300 to 420 nm with the peak intensity at 340 nm. The recorded spectrum is similar to the

Table 1 Operating conditions for the optical measurements

	T_{30}, K	P_{30}, bar (abs.)	M_{air}, kg/s	W_{fuel}, kg/h	AFR rig	ϕ rig	dp/P_{30}, %
Point 1	524 ± 0.3	3.20 ± 0.004	0.210 ± 0.004	12.38 ± 0.24	60.9 ± 1.7	0.24 ± 0.01	4.03 ± 0.11
Point 2	535 ± 0.4	3.20 ± 0.006	0.210 ± 0.003	32.58 ± 0.07	23.2 ± 0.3	0.63 ± 0.01	5.23 ± 0.19

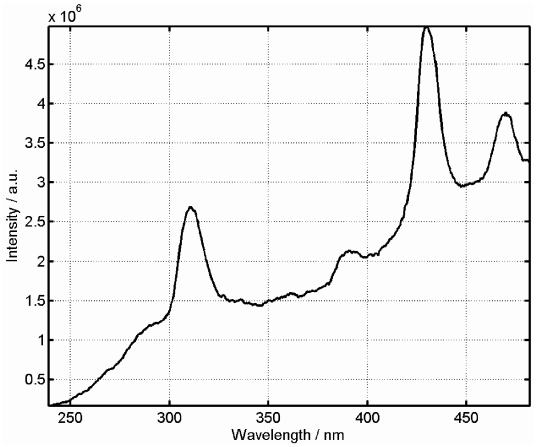

Fig. 5 Flame emission spectrum recorded for global AFR 60.

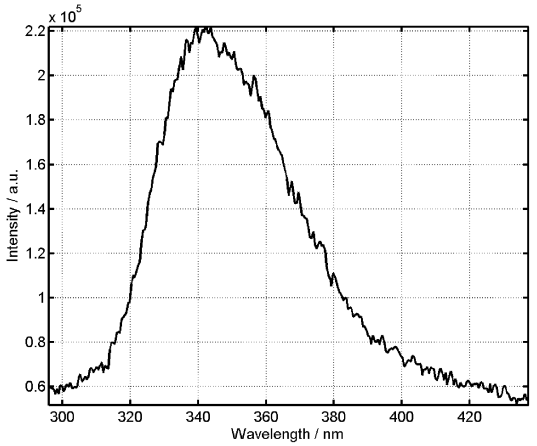

Fig. 6 Fluorescence spectrum from kerosene Jet-A, measured at running condition AFR 60.

fluorescence spectra of Jet-A vapor detected in a cell by Löfström et al. [13]. The spectrum presented in Fig. 6 has not been corrected for the wavelength sensitivity of the spectrograph/detector system.

In Figs. 7a–7c simultaneously detected single-shot pairs of Mie scattering and LIF images at the run condition of AFR 60 are presented. The duct outlet is located at the right edges of the images with the central axis located along the vertical center of the images. The flow direction is from right to left in the images and the laser sheet propagates from the bottom to the top. The signal intensities in the images are represented by a false color scale in order to distinguish between different intensity levels. In addition to the images, contours surrounding the strongest parts of the signals are shown both in the images and in a separate plot to the right of each image pair.

The strong signal detected at 532 nm arises from Mie scattering in the liquid phase of the fuel and the Mie images visualize the fuel spray cone. Comparing the individual shots it is possible to observe fluctuations in the shape of the fuel spray. When comparing the images or the contours of the two signals similarities in their shape can readily be seen. This implies that a fluorescence signal also is obtained from the liquid phase of the fuel. However, differences between the signal distributions also exist, and the fluorescence images also show a signal in regions where no corresponding Mie scattering signal appears, which indicates the presence of fuel vapor in these regions. This difference can be seen in the lower part of the three image pairs of Figs. 7a–7c, especially when comparing the extracted contours. Regions of a purely fluorescence signal exist outside the fuel spray cone, indicating vaporized fuel, which could be expected for this particular kind of flame. From symmetry considerations a similar region of fluorescence signal and fuel vapor

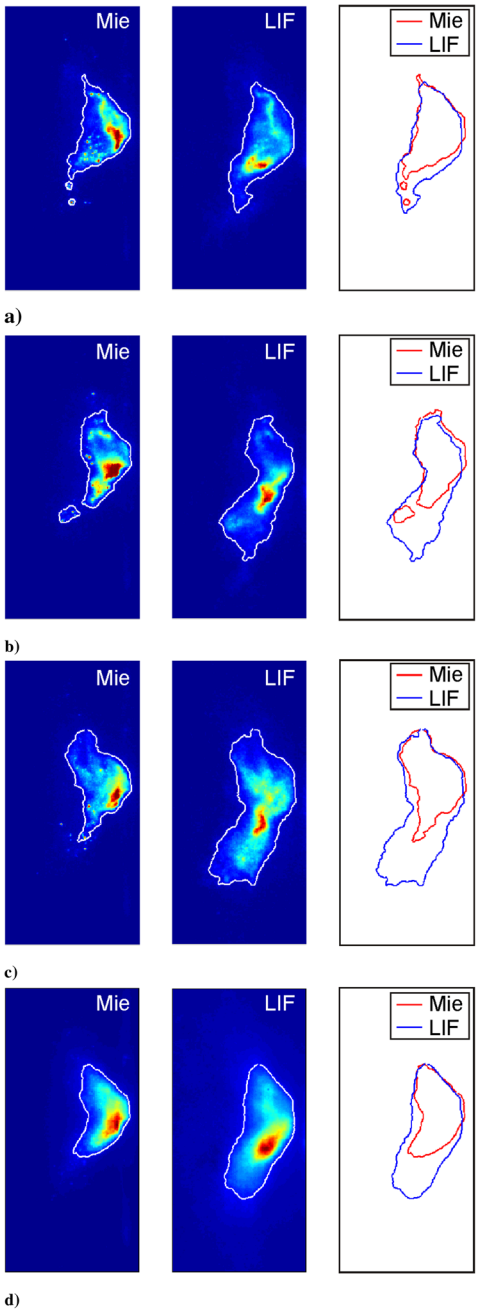

Fig. 7 Mie scattering and LIF images detected at the running condition of AFR 60 and $p = 3.2$ bar (abs.). The imaged area corresponds to 40 mm × 85 mm. The LP(P)4 duct is located along the right edge of the images. a)–c) Single-shot images of simultaneous Mie scattering (left) and LIF (middle). The contour of the signal area is indicated by the white curve in each image and the Mie scattering and fluorescence contours are also shown together in a plot (right). d) Average Mie scattering and LIF images obtained from 20 single-shot images each.

would be expected to appear outside the upper part of the spray cone in the images. Weak traces of this can also be seen in the images. Most probably, the 266 nm UV beam is strongly attenuated when passing through the liquid fuel spray. Because the laser sheet propagation is from bottom to top in the images, this would result in a weak UV beam reaching the upper region in the images, and that would explain the lack of a fluorescence signal in that region. In Fig. 7d average Mie scattering and LIF images, obtained from 20 single-shot images, are shown. The observations from the single shots of the fuel cone and the vaporized fuel can be seen also in these images.

Figure 8 shows Mie scattering and LIF data obtained at the run condition AFR 23. At this run condition, larger variations in the spray

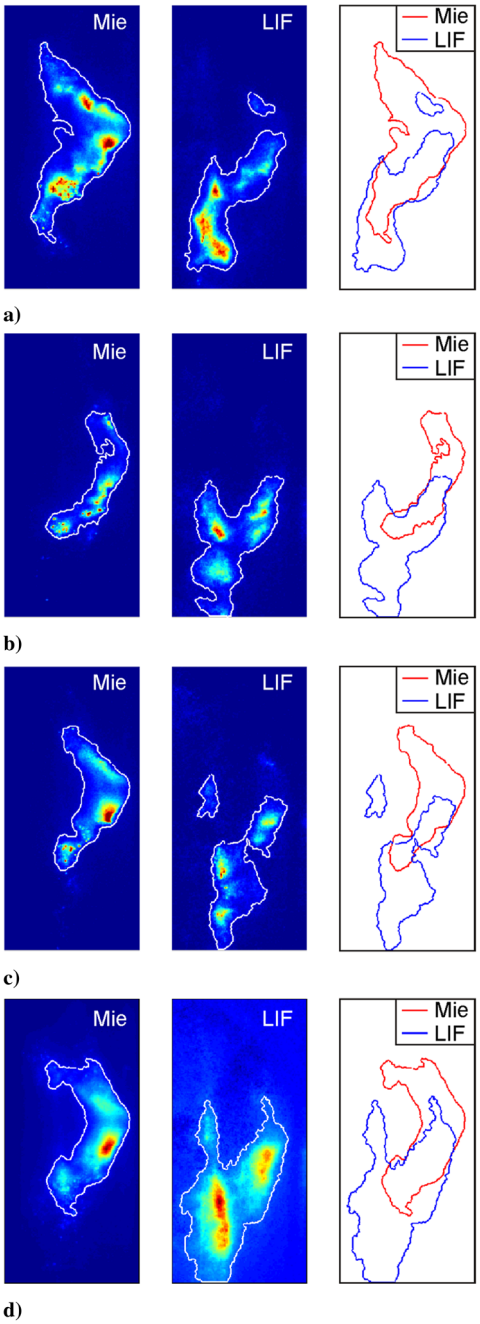

Fig. 8 Mie scattering and LIF images detected at the running condition of AFR 23 and $p = 3.2$ bar (abs.). The imaged area corresponds to 40 mm × 85 mm. The LP(P)4 duct is located along the right edge of the images. a)–c) Single-shot images of simultaneous Mie scattering (left) and LIF (middle). The contour of the signal area is indicated by the white curve in each image and the Mie scattering and fluorescence contours are also shown together in a plot (right). d) Average Mie scattering and LIF images obtained from 20 single-shot images each.

shape were encountered, which is reflected in the single-shot image pairs shown in Figs. 8a–8c. The same observations regarding the distributions of the Mie scattering and LIF signals can be made, that is, an overlap exists for regions of liquid fuel and vaporized fuel can be identified from regions showing only a fluorescence signal. The absence of a fluorescence signal in the upper part of the images is more clearly noticed for this run condition, most likely due to even stronger attenuation of the UV beam due to the presence of more liquid fuel at this air fuel ratio. In Fig. 8d the average Mie scattering and LIF signal distributions are shown. During measurements at this run condition, deposits of liquid fuel and coke accumulated on the combustion chamber windows. This attenuated and in some regions

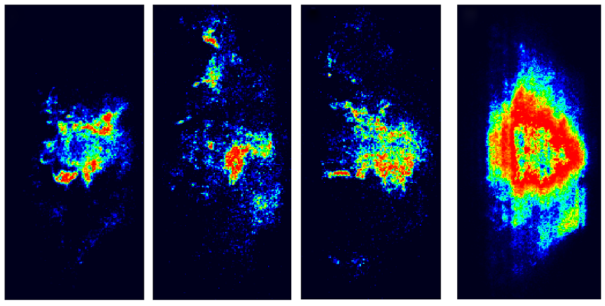

Fig. 9 Single-shot LII images a)–c) and an average image d) obtained from 50 single-shot images of the LII signal detected at AFR 60. The imaged area corresponds to 40 mm × 85 mm and the LP(P)4 duct is located along the right edge of the image.

completely blocked the signals. This problem was most severe for the detection of the fluorescence signal and can be seen in the average fluorescence image of Fig. 8d. Comparing the two run conditions it can also be seen that the fuel cone angle is wider for the case of AFR 23. The angles are 40 deg for AFR 60 and 60 deg for AFR 23. There appears to be more shot-to-shot variation in the fuel vapor distribution in Fig. 7 (AFR 60) than in Fig. 8 (AFR 23). This may be caused by the fact that the AFR 60 flow had a much lower fuel flow rate and it may have been more affected by the airflow patterns. These two-dimensional images represent instantaneous snapshots of a three-dimensional structure. It may be that some airflow precession, for example, caused variations in the fuel vapor distribution when the fuel flow rate was low. The AFR 23 case had 3 times the jet momentum of the AFR 60 case, and may not have been as strongly affected. Clearly, ideas such as this one require further investigation.

C. LII Measurements

In Fig. 9 single-shot LII images and an average image of the LII signal obtained for AFR 60 is presented. The measurement region for this image is the same as for the Mie scattering and LIF measurements. From the averaged image it can be seen that the detected signal seems to resemble the shape of the flame (see Fig. 4) with a strong incandescence from the part of the flame that appears most luminous in the photo, as one would expect. Comparing the LII image to the results from the Mie scattering and fluorescence measurements shows that the strong incandescence appears downstream of the spray cone in the immediate vicinity of the liquid fuel region. Farther away from the vertical middle of the image where vaporized fuel was detected the incandescence signal decreases, indicating combustion at leaner conditions.

D. Technique Development/Future Work

As described in the present work there is considerable potential for advanced laser diagnostic techniques even in highly applied environments. Still there seems to be further measurement requirements, for example, to visualize important combustion parameters in real time, not at the more typical 10 Hz which cannot resolve the temporal evolution of the phenomena to be studied. During the last decade we have developed a laser/detector system consisting of a cluster of double pulsed Nd:YAG lasers and a framing camera which gives the possibility for capturing up to eight 2-D images with a framing rate up to 50 MHz. Each laser in the cluster can deliver ~200 mJ at 532 nm. This system has been extensively used for studies of turbulent flames and in internal combustion (IC) engines; see, for example, [18,19].

To investigate the potential of this apparatus for simultaneous Mie scattering/fluorescence we have made further investigations and development of the method including time-resolved studies of an atmospheric pressure, laboratory scale Jet-A spray. The spray was generated by a glass nebulizer where nitrogen was blown through the liquid to form a spray. To get temporally resolved images, the experiments were performed using the high-speed system formed by

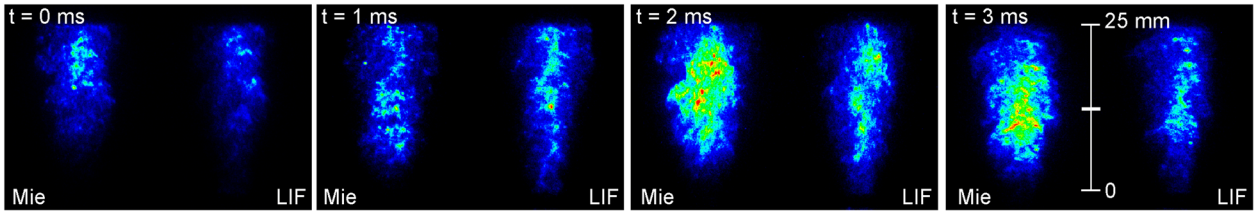

Fig. 10 Simultaneous detection of Mie scattering and LIF signal for a two-phase study in a Jet-A spray. The jet flow direction is from bottom to top in the images.

the multi-Nd:YAG laser cluster and the Hadland framing camera. The experimental setup was similar to that previously described. Because of experimental requirements two HR 266 dichroic mirrors have been included in the setup to reject the Mie scattering laser light. For this demonstration the laser cluster was used in single pulse operation giving four pulses with more or less arbitrary time separation between the pulses and where the maximum framing rate in this experiment was given by the phosphor decay of the image intensifier on the framing camera to ~1 MHz. In the experiments described here the time between the pulses was set to 1 ms. This setup thus made it possible to study the temporal and spatial evolution of the droplets during the vaporization process, giving high-speed visualization of qualitative fuel and droplet distributions. Figure 10 illustrates an example of an image sequence of Mie scattering and LIF obtained simultaneously in a Jet-A spray.

IV. Summary and Conclusions

In the present investigation optical diagnostics have been applied in a Rolls–Royce Deutschland gas turbine pilot burner. Measurements have been done in the combustion zone of the Jet-A fueled LP (P)4 module equipped with a centrally placed pilot burner. A major part of the study describes a practical industrial problem, that is, the mixing/vaporization of fuel and air. Simultaneous single-shot acquisition of Mie scattering and LIF images was performed for visualization of the liquid and gaseous phase of the fuel distribution. Despite a complicated environment for performing optical diagnostics the two-phase technique appeared to be a valuable tool for the understanding of the mixing and vaporization process for the pilot burner configuration. In the images, similarities in the spatial distribution of the Mie scattering and the LIF signals can be observed. However, isolated fuel vapor regions can be distinguished from the liquid phase regions, mainly at the outside of the spray cone. The individual single-shot images also reveal fluctuations in the shape of the fuel spray cone. This observation is more obvious for the fuel rich running condition.

Moreover, laser-induced incandescence was applied in the combustion zone of the pilot burner to obtain qualitative information on soot distribution. The LII images show structures similar to those obtained by video camera recording and Mie scattering visualization and resemble the spray shape of the duct. Furthermore, a noticeable shot-to-shot variation in soot structure is observed, most likely due to the airflow patterns in the chamber.

Spectrally resolved flame emission data originating from chemiluminescence and thermal radiation was recorded to gain information on the pilot burner combustion characteristics. In the result a combined nonpremixed and premixed behavior of the flame can be observed.

Future work might include temporally resolved LIF/Mie measurements using the multi-Nd:YAG laser system and the high-speed framing camera. High spatial resolution in combination with temporally resolved images can be used to estimate the length and time scales for evaporation and mixing with air of kerosene Jet-A for the LP(P)4 pilot burner.

Acknowledgments

This work was supported by the European Union through the project entitled Low Pollutant Combustor Technology Program (LOPOCOTEP Contract G4RD-CT-2001-00447) and via the European Union (EU) Large Scale Facility in Combustion at Lund. The authors gratefully acknowledge the work of Rutger Lorensson at Combustion Physics/Lund University for maintenance and operation of the test rig. Henrik Bladh and Per-Erik Bengtsson at Combustion Physics/Lund University are gratefully acknowledged for the discussions and support for the LII measurement.

References

[1] Lefebvre, A. H. *Gas Turbine Combustion*, Taylor and Francis, Philadelphia, PA, 1998.

[2] Bank, R. v.d., Doerr, T., Linne, M., Lindholm, A., and Guin, C., "Investigations on Internally Staged LP(P) Kerosene Injection Systems," International Symposium on Air Breathing Engines 2005-1102, 2005.

[3] Bank, R. v.d., and Schilling, T., "Development of an Ultra-Low NOx LP(P) burner," ASME GT2004-53341, 2004.

[4] Eckbreth, A. C., *Laser Diagnostics for Combustion Temperature and Species*, 2nd ed., Gordon and Breach, Amsterdam, 1996.

[5] Kohse-Höinghaus, K., and Jeffries, J. B., *Applied Combustion Diagnostics*, Taylor and Francis, New York, 2002.

[6] Schulz, C., and Sick, V., "Tracer-LIF Diagnostics: Quantitative Measurement of Fuel Concentration, Temperature and Fuel/Air Ratio in Practical Combustion Systems," *Progress in Energy and Combustion Science*, Vol. 31, No. 1, 2005, pp. 75–121.

[7] Melton, L. A., and Verdieck, J. F., "Vapor/Liquid Visualization in Fuel Sprays," *Twentieth Symposium on Combustion*, The Combustion Institute, Pittsburgh, PA, 1984, pp. 1283–1290.

[8] Ipp, W., Wagner, V., Krämer, H., Wensing, M., Leipertz, A., Arndt, S., and Jain, A. K., "Spray Formation of High-Pressure Swirl Gasoline Injectors Investigated By Two-Dimensional Mie and LIF Techniques," SAE Technical Series 1999-01-0498, 1999.

[9] Wagner, V., Ipp, W., Wensing, M., and Leipertz, A., "Fuel Distribution and Mixture Formation Inside a Direct-Injection SI Engine Investigated By 2d Mie and Lief Techniques," SAE Technical Series 1999-01-3659, 1999.

[10] Jermy, M. C., and Greenhalgh, D. A., "Planar Dropsizing by Elastic and Fluorescence Scattering in Sprays too Dense for Phase Doppler Measurement," *Applied Physics B (Lasers and Optics)*, Vol. 71, No. 5, 2000, pp. 703–710.

[11] Davy, M. H., Williams, P. A., and Anderson, R. W., "Effects of Fuel Composition on Mixture Formation in a Firing Direct-Injection Spark-Ignition (Disi) Engine: An Experimental Study Using Mie-Scattering and Planar Laser-Induced Fluorescence (Plif) Techniques," SAE Technical Series 2000-01-1904, 2000.

[12] Stojkovic, B. D., and Sick, V., "Evolution and Impingement of an Automotive Fuel Spray Investigated with Simultaneous Mie/LIF Techniques," *Applied Physics B (Lasers and Optics)*, Vol. 73, No. 1, 2001, pp. 75–83.

[13] Löfström, C., Kaaling, H., and Aldén, M., "Visualization of Fuel Distributions in Premixed Ducts in a Low-Emission Gas Turbine Combustor Using Laser Techniques," *Twenty-Sixth Symposium on Combustion*, The Combustion Institute, Pittsburgh, PA, 1996, pp. 2787–2793.

[14] Löfström, C., Engström, J., Richter, M., Kaminski, C. F., Johansson, P., Nyholm, K., Hult, J., Nygren, J., and Aldén, M., "Feasibility Studies and Application of Laer/Optical Diagnostics for Characterization of a Practical Low-Emission Gas Turbine Combustor," ASME GT2000-0124, 2000.

[15] Brown, M., Meyer, T., Gord, J., Belovich, V., and Roquemore, W., "Laser-Induced Incandescence Measurements in the Reaction Zone of a Model Gas Turbine Combustor," AIAA 2002-0393, 2002.

[16] Meier, U. E., Wolff-Gassmann, D., and Stricker, W., "LIF Imaging and 2D Temperature Mapping in a Model Combustor at Elevated Pressure," *Aerospace Science and Technology*, Vol. 4, No. 6, 2000, pp. 403–414.

[17] Meyer, T. R., Roy, S., Belovich, V. M., Corporan, E., and Gord, J. R., "Simultaneous Planar Laser-Induced Incandenscence, OH Planar Laser-Induced Fluorescence, and Droplet Mie Scattering in Swirl-Stabilized Spray Flames," *Applied Optics*, Vol. 44, No. 3, 2005, pp. 445–454.

[18] Kaminski, C. F., Hult, J., and Aldén, M., "High Repetition Rate Planar Laser Induced Fluorescence of OH in a Turbulent Non-Premixed Flame," *Applied Physics B (Lasers and Optics)*, Vol. 68, No. 4, 1999, pp. 757–760.

[19] Hult, J., Richter, M., Nygren, J., Aldén, M., Hultqvist, A., Christensen, M., and Johansson, B., "Application of a High Speed Laser Diagnostic System for Single-Cycle Resolved Imaging in IC Engines," *Applied Physics*, Vol. 41, No. 24, 2002, pp. 5002–5014.

E. Gutmark
Associate Editor